Am J Physiol Heart Circ Physiol 303: H1114–H1127, 2012.
First published August 24, 2012; doi:10.1152/ajpheart.00300.2011.

Treatment with *N*-acetyl-seryl-aspartyl-lysyl-proline prevents experimental autoimmune myocarditis in rats

Pablo Nakagawa,[1]* Yunhe Liu,[1]* Tang-Dong Liao,[1] Xiaojuan Chen,[1] Germán E. González,[1] Kevin R. Bobbitt,[2] Derek Smolarek,[1] Ed L. Peterson,[2] Ross Kedl,[3] Xiao-Ping Yang,[1] Nour-Eddine Rhaleb,[1] and Oscar A. Carretero[1]

[1]*Hypertension and Vascular Research Division, Department of Internal Medicine, Henry Ford Hospital, Detroit, Michigan;* [2]*Department of Biostatistics and Research Epidemiology, Henry Ford Hospital, Detroit, Michigan; and* [3]*Integrated Department of Immunology, University of Colorado Denver and National Jewish Health, Denver, Colorado*

Submitted 25 March 2011; accepted in final form 19 August 2012

Nakagawa P, Liu Y, Liao TD, Chen X, González GE, Bobbitt KR, Smolarek D, Peterson EL, Kedl R, Yang XP, Rhaleb NE, Carretero OA. Treatment with *N*-acetyl-seryl-aspartyl-lysyl-proline prevents experimental autoimmune myocarditis in rats. *Am J Physiol Heart Circ Physiol* 303: H1114–H1127, 2012. First published August 24, 2012; doi:10.1152/ajpheart.00300.2011.—Myocarditis is commonly associated with cardiotropic infections and has been linked to development of autoimmunity. *N*-acetyl-seryl-aspartyl-lysyl-proline (Ac-SDKP) is a naturally occurring tetrapeptide that prevents inflammation and fibrosis in hypertension and other cardiovascular diseases; however, its effect on autoimmune-mediated cardiac diseases remains unknown. We studied the effects of Ac-SDKP in experimental autoimmune myocarditis (EAM), a model of T cell-mediated autoimmune disease. This study was conducted to test the hypothesis that Ac-SDKP prevents autoimmune myocardial injury by modulating the immune responses. Lewis rats were immunized with porcine cardiac myosin and treated with Ac-SDKP or vehicle. In EAM, Ac-SDKP prevented both systolic and diastolic cardiac dysfunction, remodeling as shown by hypertrophy and fibrosis, and cell-mediated immune responses without affecting myosin-specific autoantibodies or antigen-specific T cell responses. In addition, Ac-SDKP reduced cardiac infiltration by macrophages, dendritic cells, and T cells, pro-inflammatory cytokines [interleukin (IL)-1α, tumor necrosis factor-α, IL-2, IL-17] and chemokines (cytokine-induced neutrophil chemoattractant-1, interferon-γ-induced protein 10), cell adhesion molecules (intercellular adhesion molecule-1, L-selectin), and matrix metalloproteinases (MMP). Ac-SDKP prevents autoimmune cardiac dysfunction and remodeling without reducing the production of autoantibodies or T cell responses to cardiac myosin. The protective effects of Ac-SDKP in autoimmune myocardial injury are most likely mediated by inhibition of *1*) innate and adaptive immune cell infiltration and *2*) expression of proinflammatory mediators such as cytokines, chemokines, adhesion molecules, and MMPs.

N-acetyl-seryl-aspartyl-lysyl-proline; experimental autoimmune myocarditis; cardiac hypertrophy; cardiac dysfunction; $CD4^+$ T helper lymphocytes; delayed-type hypersensitivity

MYOCARDITIS IS AN INFLAMMATORY disease of the heart muscle commonly associated with cardiotropic infections and has been linked to development of autoimmunity. Myocarditis-induced dilated cardiomyopathy is a significant cause of sudden death in young adults (5) and in 30% of cases can progress to heart failure, a major cause of morbidity and mortality among young adults with a 10-year survival rate of <40% (4, 23). *N*-acetyl-seryl-aspartyl-lysyl-proline (Ac-SDKP) is a naturally occurring tetrapeptide released from thymosin β_4 by prolyl oligopeptidase (7). Ac-SDKP is hydrolyzed almost exclusively by angiotensin-converting enzyme (ACE), and its plasma concentration is increased by ACE inhibitors (2, 7). The anti-inflammatory and anti-fibrotic effects of ACE inhibitors are known to be mediated in part by Ac-SDKP (28, 30). Hearts from rats overexpressing ACE have lower Ac-SDKP concentrations and increased fibrosis (31). Treatment with Ac-SDKP reduces cardiac inflammation and fibrosis in hypertension and in heart failure postmyocardial infarction (MI) (27, 29, 34, 44). In rats with myocarditis induced by intrapericardiac galectin-3 (a proinflammatory lectin released by macrophages), Ac-SDKP prevented cardiac inflammation, fibrosis, hypertrophy, and dysfunction (24); on the other hand, in hypertension and MI, Ac-SDKP reduced both inflammation and fibrosis but failed to decrease hypertrophy or improve cardiac dysfunction (8, 29, 34, 44). While these data suggest Ac-SDKP protects against cardiac damage due to pressure overload or local inflammatory responses, we still do not know whether it prevents autoimmune-induced cardiovascular diseases. To answer this question, we studied experimental autoimmune myocarditis (EAM) in rats, an animal model of human myocarditis (18). In this condition and also many other autoimmune diseases as well as chronic inflammation, infiltration by macrophages, dendritic cells, and T helper cells is a significant component of the process (37). Proinflammatory cytokines, chemokines, cell adhesion molecules, and matrix metalloproteinases (MMP) are all necessary for development of EAM (12, 16, 33). We tested the hypothesis that Ac-SDKP prevents autoimmune myocardial injury by modulating immune responses.

MATERIALS AND METHODS

Animals. Seven-week-old male Lewis rats (Charles River, Wilmington, MA) were housed in an air conditioned room with a 12:12-h light-dark cycle and given standard rat chow (0.4% sodium) and tap water. They were allowed 7 days to adjust to their new environment. Before all surgical procedures, butorphanol (2 mg/kg sc) was used to induce analgesia and pentobarbital sodium (50 mg/kg ip) for anesthesia. All protocols were approved by the Institutional Animal Care and Use Committee of Henry Ford Hospital.

Induction of EAM. EAM was induced in Lewis rats following Kitabayashi's protocol (17). All rats were immunized at the beginning of the experiment (*day 0*) and again 7 days later (*day 7*). In each immunization, rats were anesthetized and intradermically injected with 1 mg of porcine cardiac myosin (Sigma, St. Louis, MO) emulsified with an equal volume of complete Freund's adjuvant (CFA) supplemented with *Mycobacterium* tuberculosis H37RA.

* P. Nakagawa and Y. Liu contributed equally to this work.

Address for reprint requests and other correspondence: O. A. Carretero, Hypertension and Vascular Research Division, 2799, W. Grand Blvd., Detroit, MI 48202 (e-mail: ocarret1@hfhs.org).

Experimental protocols. Rats were randomly divided into the following four groups: *1*) controls, injected with CFA and infused with saline using an osmotic minipump (Alzet); *2*) Ac-SDKP, injected with CFA and infused with Ac-SDKP (800 $\mu g \cdot kg^{-1} \cdot day^{-1}$); *3*) EAM, injected with emulsified porcine myosin in CFA and infused with saline; and *4*) EAM + Ac-SDKP, injected with emulsified porcine myosin in CFA and infused with Ac-SDKP (800 $\mu g \cdot kg^{-1} \cdot day^{-1}$). Ac-SDKP infusion was started at *day 0*. Rats were killed at different time points depending on the parameter studied. At 2 wk postimmunization, we measured MMP activity. At 3 wk, total leukocyte infiltration, delayed-type hypersensitivity (DTH), autoantibody titers, antigen-specific T cell responses, T helper cell intracellular cytokines, dendritic cell infiltration, and myocardial expression of cytokines, chemokines, and adhesion molecules were measured. At 4 wk, we measured organ weight, blood pressure, cardiac function, collagen deposition, macrophage and T cell infiltration, and MMP activity.

Blood pressure and echocardiography. Systolic blood pressure (SBP) was measured by tail cuff in nonanesthetized rats before and 4 wk after immunization. After anesthetizing the rats, echocardiography and Doppler sonography using an Acuson Sequoia C 256 with a 15-MHz transducer were performed together with electrocardiography before and 4 wk after immunization. M-mode echocardiography was conducted first in the parasternal long-axis view to measure left ventricle (LV) dimensions and then in the anterior short-axis view to evaluate LV ejection fraction (LVEF). Transmitral Doppler inflow waves were used to measure peak early diastolic filling velocity (E wave), peak filling velocity at atrial contraction (A wave), and the ratio between them (E/A), assessing diastolic function as described previously (32). After determining the aortic root dimension (AoD) and systolic velocity-time integral (VTI), stroke volume was calculated according to the formula: stroke volume = $(VTI)[(AoD/2)^2]$ and cardiac output (CO) using the formula: CO = stroke volume × heart rate (HR). All Doppler spectra were recorded for five to seven cardiac cycles at a sweep speed of 200 mm/s.

Heart, lung, liver, kidney, thymus, and spleen weight. Four weeks after immunization, the rats were anesthetized and the heart stopped during diastole by injecting 15% potassium chloride solution, then excised, weighed, and expressed as the ratio of heart weight (HW) to body weight (BW). The lungs, liver, kidney, thymus, and spleen were also removed and weighed.

Histology. The LV was sectioned transversely into four slices from apex to base. The two middle slices (biventricular cross sections) were used for histological and immunohistochemical studies, and the base and apex were used for protein analysis. Five-micrometer sections were fixed in 10% formalin, embedded in paraffin, and inflammation estimated using hematoxylin-eosin staining. Sections were analyzed blindly by two investigators, and the extent of myocardial inflammation was graded according to the following four-tier system: *grade 1* corresponding to cardiac necrosis/infiltration up to 10% of the cardiac section; *grade 2*, 11–20%; *grade 3*, 21–40%; and *grade 4*, >40% (43). Myocardial interstitial and perivascular collagen deposition, both markers of fibrosis, were quantified using picrosirius red (40). Microphotographs were taken at ×400 magnification using an Olympus IX81 microscope (Olympus America, Center Valley, PA) and DP70 digital camera. At least 100 images of the surface of each section were analyzed with an Olympus Microsuite Biological system. Interstitial collagen deposition was assessed by calculating the ratio of collagen to the entire section. Perivascular collagen was measured as the ratio of the surrounding fibrotic area to total vessel area. All measurements and analyses were carried out in a blind fashion.

DTH assay. Myosin DTH was quantified 3 wk after immunization based on swelling of the ear as described by Godsel et al. (11). Ear thickness was measured with a micrometer (serial no. 7323; Mitutoyo MTI, Aurora, IL). Ten micrograms of myosin in a solution of 0.16 M K_2PO_4, 0.01 M $Na_4P_2O_7$, and 0.3 M KCl (*p*H 6.8) were injected intradermically into the dorsal surface of the ear using a 50- to 100-μl glass Hamilton syringe fitted with a 30-gauge needle, whereas 10 μg BSA in the same solution was injected in the opposite ear as a control. After 24 h, net swelling of the control ear (mm) was subtracted from the myosin-treated ear.

Anti-cardiac myosin autoantibody assay. Myosin-specific antibodies in the serum were measured by enzyme-linked immunosorbent assay (ELISA) 3 wk postimmunization as described by Wang et al. (42). Flat-bottom 96-well ELISA plates were coated with porcine cardiac myosin (10 μg/ml) by incubating them overnight at 4°C. After washing the plates two times with 0.05% PBS-Tween and blocking them with 1% BSA in PBS, serum diluted 1:5,000 was first incubated overnight at 4°C; then goat anti-rat IgG conjugated to alkaline phosphatase (Sigma) was added, and samples were incubated for 1 h at room temperature and washed with PBS-Tween. Finally, paranitrophenylphosphate (Sigma) was added, halting the reaction at 10 min by adding 1 M sodium hydroxide and measuring optical density (OD) at 405 nm. Each sample was analyzed in duplicate.

Antigen-specific T cell proliferation and intracellular cytokines. Cells were collected from inguinal and popliteal draining lymph nodes 3 wk postimmunization, resuspended in prewarmed PBS/0.1% BSA at a final concentration of 1×10^6 cells/ml, and incubated with carboxyfluorescein diacetate, succinimidyl ester (CFSE) at a final concentration of 10 μM for 10 min. After the cells were washed two times with PBS, they were resuspended in T cell medium (RPMI 1640 containing 10% FBS, 50 μM 2-mercaptoethanol, 100 U/ml penicillin, and 100 μg/ml streptomycin) and placed in 96-well microtiter plates (Corning-Costar) preloaded with 5×10^5 irradiated syngenic splenocytes pulsed with 50 μg/ml cardiac myosin for 24 h. Samples were incubated with 50 μg/ml porcine cardiac myosin for 6 days at 37°C in a humidified atmosphere containing 5% CO_2. After incubation, cells were stained with antibodies [APC-Cy7 anti-CD45, OX-1 (BioLegend); PE-Cy7 anti-CD8, OX-8 (eBioscience); PE-Cy5 anti-CD4, OX-35 (BD Biosciences); APC anti-CD25, OX-39 (eBioscience)] and fixed with 1% paraformaldehyde at room temperature for 20 min. Samples were analyzed using an LSR II flow cytometer (BD Biosciences) and Fluorescence-activated cell sorting (FACS) Diva software (version 6.1.3). Cell proliferation was calculated as the percentage of $CD45^+$, $CD4^+$, and $CD25^+$ gated cells with reduced CFSE fluorescence intensity. For intracellular cytokine assay, 1×10^6 lymph node cells were stimulated with 80 ng/ml phorbol 12-myristate 13-acetate plus 1 μg/ml ionomycin and 20 ng/ml brefeldin A for 4 h at

Table 1. *Effect of Ac-SDKP on heart rate and organ weight measured 4 wk after immunization*

	Control	Ac-SDKP	EAM	EAM + Ac-SDKP
BW, g	325 ± 4 (12)	326 ± 4 (12)	305 ± 8 (13)	321 ± 8 (14)
Lungs/BW, mg/100 g	338 ± 22 (12)	367 ± 8 (12)	430 ± 16* (13)	377 ± 8.6# (14)
Liver/BW, g/100 g	3.66 ± 0.11 (8)	3.66 ± 0.16 (8)	3.79 ± 0.14 (10)	3.58 ± 0.08 (9)
Thymus/BW, mg/100 mg	137 ± 6 (12)	141 ± 7 (12)	165 ± 11* (14)	140 ± 6 (13)
Spleen/BW, mg/100 g	174 ± 7 (6)	182 ± 6 (6)	174 ± 5 (8)	174 ± 8 (7)
Kidney/BW, g/100 g	0.86 ± 0.06 (9)	0.81 ± 0.02 (12)	0.89 ± 0.05 (8)	0.81 ± 0.02 (7)

Values are means ± SE; nos. in parentheses are no. of animals analyzed/group. Ac-SDKP, *N*-acetyl-seryl-aspartyl-lysyl-proline; EAM, experimental autoimmune myocarditis; BW, body wt. *$P < 0.05$, EAM vs. control. #$P < 0.05$, EAM + Ac-SDKP vs. EAM.

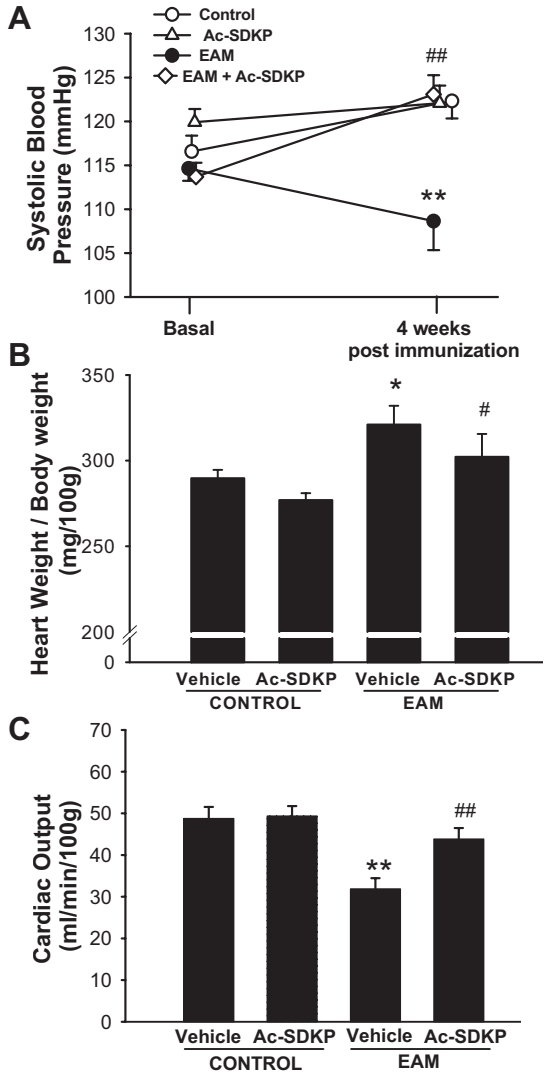

Fig. 1. *A*: systolic blood pressure measured by tail cuff at the beginning and end of the experiment (4 wk after immunization) in controls and experimental autoimmune myocarditis (EAM) rats treated with vehicle or *N*-acetyl-seryl-aspartyl-lysyl-proline (Ac-SDKP) (n = 12–14). *B*: heart weight corrected by body weight (an indicator of hypertrophy) measured 4 wk after immunization in controls and EAM rats treated with vehicle or Ac-SDKP (n = 11–13). *C*: cardiac output measured by echocardiography 4 wk after immunization in controls and EAM rats treated with vehicle or Ac-SDKP (n = 11–14). *$p <$ 0.01 and **$p < 0.001$, EAM + vehicle vs. control + vehicle. #$p < 0.05$ and ##$p < 0.001$, EAM + Ac-SDKP vs. EAM + vehicle.

37°C and then washed, stained for surface markers, fixed with 1% paraformaldehyde at room temperature for 20 min, and resuspended in permeabilization buffer. Intracellular markers were stained with a series of antibodies: FITC anti-interferon (IFN)-γ, DB-1 (Biolegend); PE anti-interleukin (IL)-4, OX-81 (BD Biosciences); and PerCp-Cy5.5 anti-IL-17, Tc11 (Biolegend). A BD Biosciences LSR II flow cytometer was used for all analyses.

Immunohistochemical staining. Six-micrometer frozen sections were immunostained with the appropriate antibody: anti-CD45 (total leukocytes), ED-1 (monocytes/macrophages), CD11c (dendritic cells), CD4 (T helper cells), or CD8 (T cytotoxic cells). Negative controls were processed in a similar fashion but were not treated with the primary antibody. Positive cells (red/dark brown staining) with clearly visible nuclei were counted in high-power fields and expressed as cells per square millimeter (9). All measurements and analyses were carried out in a blind fashion.

Proteomic array. Cross sections of the heart were homogenized in lysis buffer (PBS containing 1% Triton X-100, 10 μg/ml aprotinin, 10 μg/ml leupeptin, and 10 μg/ml pepstatin). Protein levels of 29 inflammatory mediators were measured in tissue homogenates using a proteomic array kit (R&D Biosciences, Minneapolis, MN); these included IL-1α and -β, tumor necrosis factor (TNF)-α, IL-2, interferon-γ-induced protein 10 (IP-10), cytokine-induced neutrophil chemoattractant-1 (CINC-1), macrophage inflammatory protein (MIP)-1α, intercellular adhesion molecule (ICAM)-1, and L-selectin. Data were expressed as arbitrary units (AU) representing the OD of the protein divided by the positive control.

Western blotting. Twenty micrograms of protein from heart extracts were subjected to 10% SDS-polyacrylamide gel electrophoresis (Invitrogen, Carlsbad, CA) under reducing conditions and transferred to polyvinylidene difluoride membranes (GE Healthcare, Piscataway, NJ). Each membrane was blocked with 5% nonfat milk for 1 h and incubated with anti-rat ICAM-1 (1:500; R&D Systems, Minneapolis, MN) or anti-GAPDH (1:50,000; Cell Signaling Technology, Danvers, MA) overnight at 4°C. The membranes were incubated for 60 min with the appropriate peroxidase-conjugated secondary antibody diluted 1:20,000 (Santa Cruz Technology, Santa Cruz, CA). ECL-plus chemiluminescence detection system reagents (Amersham Biosciences, Piscataway, NJ) to visualize the bands and Films were scanned with an Epson Perfection 3200 (Epson America, Long Beach, CA).

Metalloproteinase-2 and -9 activity in cardiac tissue homogenates. Gelatin zymography was performed 2 and 4 wk postimmunization as described by Zibadi et al. (45). Ten milligrams of cardiac tissue were washed with ice-cold saline and homogenized in 0.5 ml extraction buffer (pH 5.0) containing 10 mM cacodylic acid, 150 mM NaCl, 20 mM $ZnCl_2$, 1.5 mM NaN_3, and 0.01% Triton X-100. The homogenate was centrifuged, and the supernatant was applied to 10% polyacrylamide gel zymograms (Novex, Frankfurt, Germany). After electrophoresis at 125 V and 4°C for 90 min, the gels were washed two times with renaturing buffer (2.5% Triton X-100) at room temperature for 30 min. The zymograms were then transferred to activity buffer (50 mM Tris·HCl, pH 8.0, 5 mM $CaCl_2$, 0.2 M NaCl, and 0.02% Brij-35)

Table 2. *Effect of Ac-SDKP on echocardiographic parameters measured 4 wk after immunization in rats with EAM*

	Control (n = 12)	Ac-SDKP (n = 11)	EAM (n = 14)	EAM + Ac-SDKP (n = 13)
PWT, mm	1.58 ± 0.06	1.65 ± 0.04	1.88 ± 0.08**	1.60 ± 0.06###
LV mass, (mm^3)/100 g BW	201 ± 7	200 ± 6	247 ± 18*	188 ± 7###
SF, %	58.0 ± 1.4	58.7 ± 1.2	50.2 ± 1.6*	55.4 ± 1.3#
LVEF, %	81.5 ± 0.9	83.3 ± 0.6	66.7 ± 2.6**	77.8 ± 2.5###
E/A ratio	1.49 ± 0.04	1.45 ± 0.05	1.21 ± 0.07**	1.47 ± 0.04##
HR, beats/min	379 ± 10 (12)	383 ± 12 (11)	395 ± 9 (14)	388 ± 9 (13)

Values are means ± SE; n, no. of animals analyzed/group. PWT, posterior wall thickness; LV, left ventricle; BW: body weight; SF, shortening fraction; LVEF, ejection fraction; E/A, peak early diastolic filling velocity (E)/peak filling velocity at atrial contraction (A); HR: heart rate. *$P < 0.005$ and **$P < 0.001$, EAM vs. control. #$P < 0.05$, ##$P < 0.005$, and ###$P < 0.001$, EAM + Ac-SDKP vs. EAM.

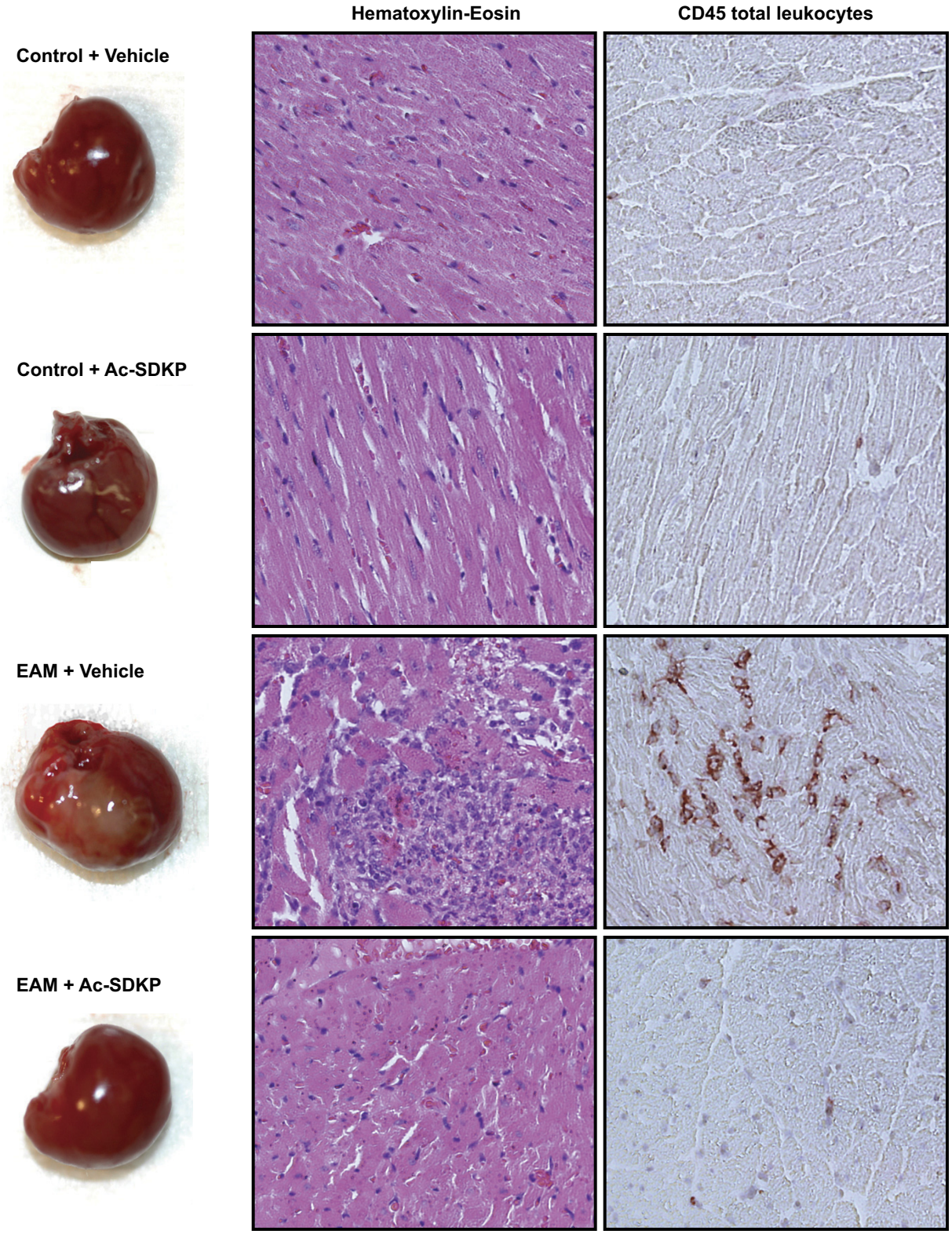

Fig. 2. *Left*: representative photographs of whole hearts taken 3 wk after immunization in controls and EAM rats treated with vehicle or Ac-SDKP. *Center*: representative images of heart sections stained with hematoxylin and eosin 3 wk after immunization in controls and EAM rats treated with vehicle or Ac-SDKP. *Right*: representative images of myocardial leukocyte infiltration (red: $CD45^+$) 3 wk after immunization in controls and EAM rats treated with vehicle or Ac-SDKP.

and developed at 37°C for 12 h. After fixation and staining with Coomassie Brilliant blue G-250 (0.25%), the zymograms were destained with 10% (vol/vol) acetic acid, and bands were quantified by image analysis.

Data analysis. All data are expressed as means ± SE. Statistical significance of the data was analyzed by Kruskall-Wallis test followed by a Wilcoxon two-sample analysis or by ANOVA followed by Tukey's test. A value of $P < 0.05$ was considered significant.

RESULTS

BW and organ weight. There were no significant differences in BW among groups 4 wk after immunization; however, lung and thymus weight both increased in rats with EAM. Ac-SDKP prevented the increase in lung weight but had no effect on the controls. Liver, spleen, and kidney weight were similar in all groups (Table 1).

SBP and cardiac function (echocardiography). By *week 4*, SBP was significantly decreased in the EAM group. Ac-SDKP prevented this decrease but had no effect on the controls (Fig. 1*A*). HW corrected by BW was significantly higher in the EAM group, but this increase was prevented by Ac-SDKP, whereas the control group showed no change (Fig. 1*B*). Rats with EAM had a significantly lower CO that was prevented by Ac-SDKP,

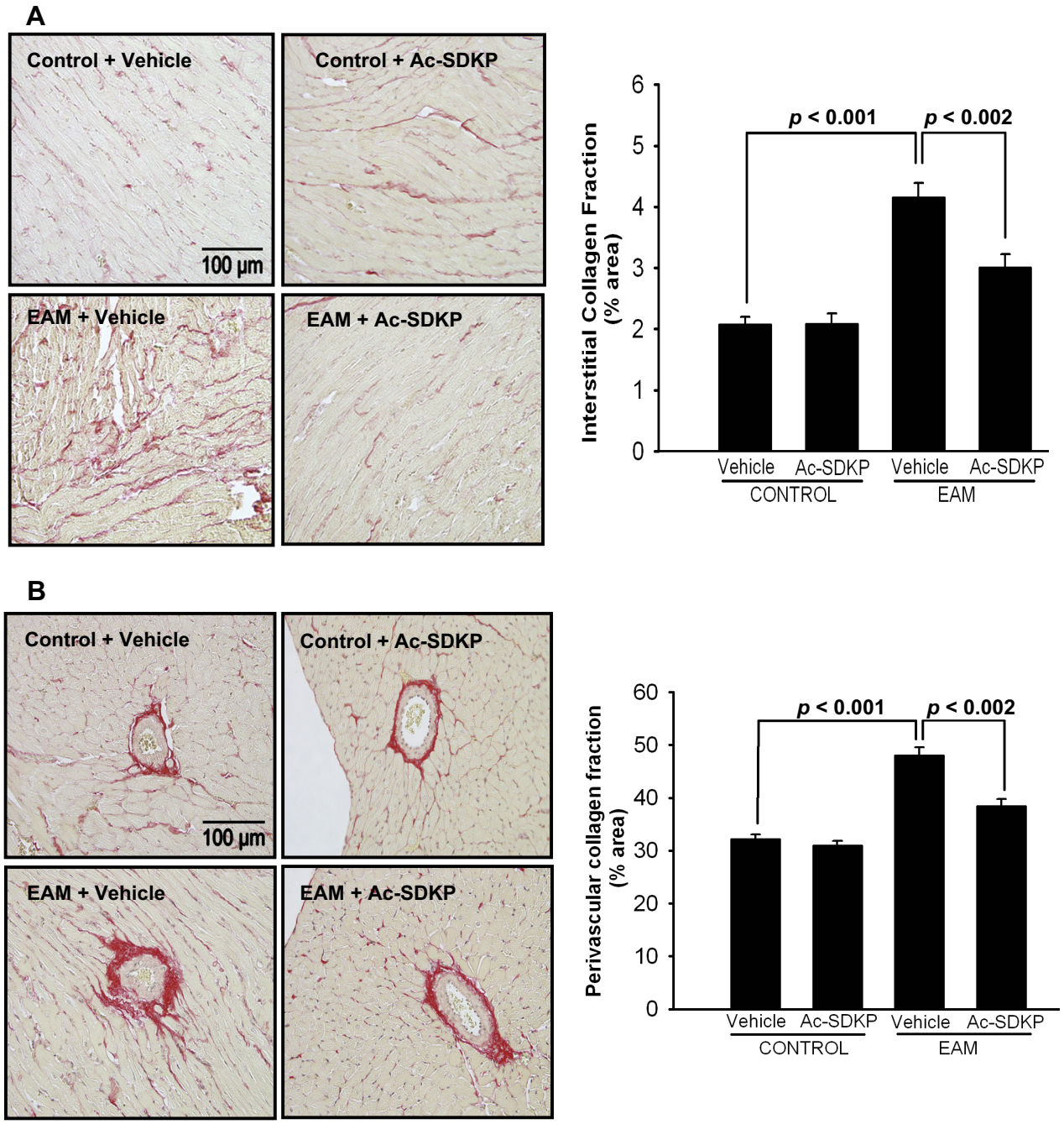

Fig. 3. *Left*: myocardial interstitial (*A*) and perivascular (*B*) collagen deposition measured by picrosirius red staining 4 wk after immunization in controls and EAM rats treated with vehicle or Ac-SDKP. *Right*: quantitative data on interstitial (*A*) and perivascular (*B*) fibrosis, expressed as a percentage of the fibrotic area (n = 12–14). NS, not significant.

whereas the controls once again showed no change (Fig. 1*C*). In addition, LV mass and posterior wall thickness increased in the EAM group while LVEF, shortening fraction, and the ratio of transmitral Doppler E (early LV filling phase)- to A (atrial contraction phase)-wave, an indicator of LV diastolic function, all decreased; and these abnormalities were prevented by Ac-SDKP. There were no differences in HR among groups (Table 2).

Macroscopic and microscopic evaluation of the heart. By *week 3*, discolored areas were observed in the hearts of EAM + vehicle but not EAM + Ac-SDKP or controls (Fig. 2, *left*). Only one rat in the EAM group had pericardial effusion. Microscopic examination revealed inflammatory loci only in the EAM group (Fig. 2, *center*). Inflammatory score was increased in EAM compared with controls (EAM 2.20 ± 0.02 vs. control 1.14 ± 0.02 AU, $p < 0.001$), and this increase was significantly reduced in EAM + Ac-SDKP (EAM + Ac-SDKP: 1.49 ± 0.14 AU, $p < 0.05$ vs. EAM) (Fig. 2, *center*). The EAM group also showed increased infiltration by $CD45^+$ leukocytes compared with the controls (319.3 ± 68.7 vs. 42.4 ± 3.2 cells/mm^2; $p < 0.001$), and this increase was partially prevented by Ac-SDKP (146.1 ± 54.5 vs. 319.3 ± 68.7 cells/mm^2; $p < 0.05$ vs. EAM). Ac-SDKP had no effect on the controls (48.5 ± 5.1 cells/mm^2) (Fig. 2, *right*).

Cardiac interstitial and perivascular collagen. By *week 4*, cardiac interstitial and perivascular collagen deposition were both higher in the EAM group; this increase was prevented by Ac-SDKP, but it had no effect on the controls (Fig. 3, *A* and *B*).

DTH. Three weeks after immunization, we measured DTH by injecting cardiac myosin in the left ear, treating the right ear with an irrelevant protein (BSA) as a control. Whereas the right ear showed no change, a swollen red nodule was seen in the left ear of the EAM group. This increase in DTH was prevented by Ac-SDKP (Fig. 4*A*).

Anti-cardiac myosin autoantibody assay. At 3 wk, serum samples from rats with EAM showed increased autoantibodies. Ac-SDKP failed to prevent this increase and had no effect on the controls (Fig. 4*B*).

Antigen-specific T cell proliferation and intracellular cytokines. By *week 3*, incubation of lymph node cells with antigen (cardiac myosin) induced proliferation of T helper cells in the rats with EAM but not in the controls, and this increase was not prevented by Ac-SDKP (Fig. 5). Intracellular FACS analysis revealed that the Th2 subset (IL-4 positive) tended to increase in EAM rats treated with either vehicle or Ac-SDKP (although the difference was not statistically significant), whereas the Th1 subset (IFN-γ positive) remained unaffected. Three out of five rats in the EAM group had increased Th17 (IL-17 positive). Although EAM and EAM + Ac-SDKP were not significantly different, none of the rats in the EAM + Ac-SDKP group had increased levels of Th17 (Fig. 6).

Cardiac infiltration by macrophages, dendritic cells, T helper cells, and cytotoxic T cells. Myocardial ED-1-positive macrophages, $CD4^+$ T helper cells, and $CD8^+$ cytotoxic T cells were all increased in the EAM group at *week 4*, whereas CD11c-positive dendritic cells were significantly increased by 3 wk. Ac-SDKP prevented all of these increases save for the cytotoxic T cells but had no effect on the controls (Figs. 7 and 8).

Expression of proinflammatory cytokines and cell adhesion molecules. By *week 3*, cardiac protein expression of cytokines related to both innate (IL-1α, TNF-α) and adaptive (IL-17)

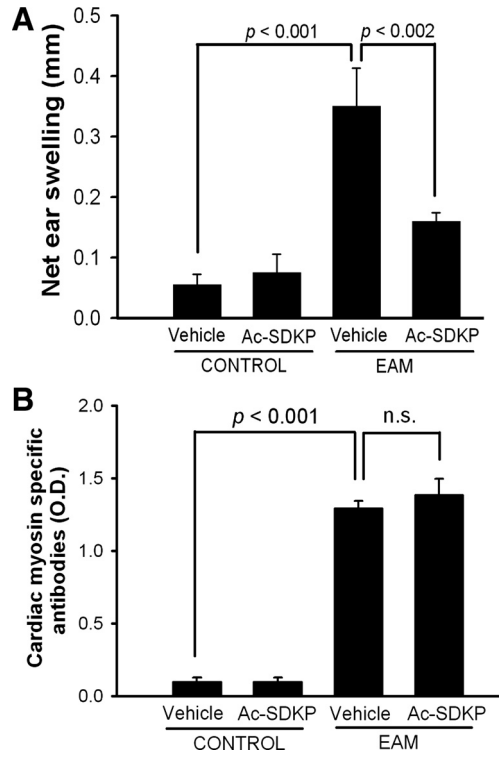

Fig. 4. *A*: delayed-type hypersensitivity to porcine cardiac myosin measured 3 wk after immunization (expressed as mm of net ear swelling) in controls and EAM rats treated with vehicle or Ac-SDKP ($n = 4–6$). *B*: cardiac myosin-specific autoantibodies measured by enzyme-linked immunosorbent assay (ELISA) in serum samples collected 3 wk after immunization ($n = 3$).

immune responses as well as chemokines (CINC-1 and IP-10) was increased in the EAM group but prevented by Ac-SDKP. Ac-SDKP also lowered IL-2, which was not significantly increased in the EAM group (Fig. 9). Cell adhesion molecules L-selectin and ICAM-1 were also increased in the EAM rats and prevented by Ac-SDKP (Fig. 10*A*). Western blots of ICAM-1 protein showed similar results (Fig. 10*B*). Other inflammatory mediators such as CINC-3, IL-1β, IL-1ra, IL-6, LIX, MIP-1α, thymus chemokine, and tissue inhibitor of MMP-1 were also increased in the EAM group and prevented by Ac-SDKP (see Table 3). Ac-SDKP had no effect on any inflammatory mediators in the control group.

Metalloproteinase-2 and -9 activity. By *week 2*, both MMP-2 and MMP-9 activity in the myocardium was higher in the EAM group, and Ac-SDKP prevented this increase (Fig. 11). However, MMP-9 returned to normal by *week 4*, whereas MMP-2 was undetectable (data not shown).

DISCUSSION

In Lewis rats immunized with cardiac myosin, Ac-SDKP prevented hypotension, cardiac remodeling (hypertrophy, inflammation, and fibrosis), and dysfunction. Using models of hypertension and MI, we showed that Ac-SDKP decreased cardiac macrophage infiltration, transforming growth factor-β expression, and fibrosis; however, it did not improve cardiac function or decrease hypertrophy (44). We also induced myocarditis by intrapericardial infusion of galectin-3 and found that Ac-SDKP not only lessened fibrosis and inflammation but also prevented cardiac dysfunction and hypertrophy (24). The ob-

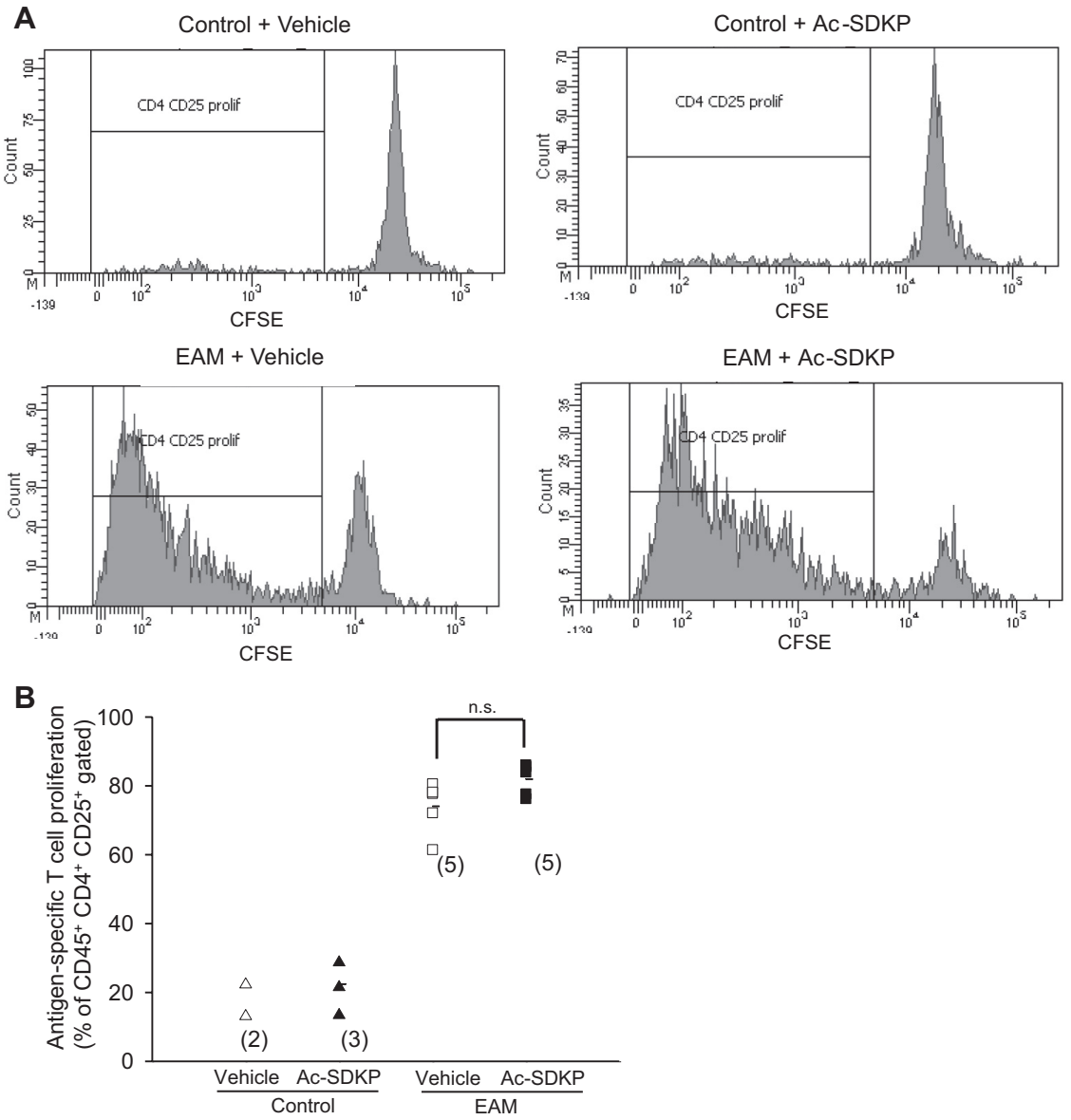

Fig. 5. *A*: representative histograms showing T helper cell proliferation in response to cardiac myosin in controls and EAM rats treated with vehicle or Ac-SDKP. Proliferation of T helper cells was seen as reduced carboxyfluorescein diacetate, succinimidyl ester (CFSE) fluorescence intensity on flow cytometry. *B*: quantitative data, expressed as %proliferating cells out of gated cells: $CD45^+$, $CD4^+$, and $CD25^+$, which are markers of total leukocytes, T helper cells, and T cell activation, respectively.

servation that Ac-SDKP improved cardiac remodeling and function in galectin-3-induced myocarditis and EAM but not in hypertension and MI is probably related to the etiology and pathogenesis of remodeling and dysfunction. EAM is considered a T cell-mediated autoimmune disease (19), and the mechanism of cardiac damage differs from galectin-3-induced myocarditis. Galectin-3 is a lectin released by macrophages that induces local inflammation when infused in the pericardium, whereas EAM is induced by immunization with cardiac myosin, which causes the immune system to react against the heart's own proteins; thus, in contrast to galectin-3-induced myocarditis, the autoimmune reaction observed in EAM depends on activation of not only the innate but also the adaptive immune system. We believe the findings presented here demonstrate for the first time that Ac-SDKP affords cardioprotection in a model of autoimmune-mediated heart disease. Four weeks after immunization, rats with EAM had significantly lower SBP, possibly because of reduced CO. Ac-SDKP prevented the decreases in both BP and CO, further supporting the hypothesis that the drop in SBP may have been secondary to decreased cardiac function. Yet, even with lower SBP, the rats with EAM had cardiac hypertrophy, suggesting that the remodeling and dysfunction were due to an autoimmune reaction independent of afterload. In immunized rats, echocardiography showed that Ac-SDKP prevented both systolic and diastolic function from decreasing while posterior wall thickness and LV mass were reduced, suggesting that Ac-SDKP prevented autoimmune-induced hypertrophy; moreover, both the lung congestion and HW corrected by BW support these observations. Therefore, we conclude that, in autoimmune-mediated

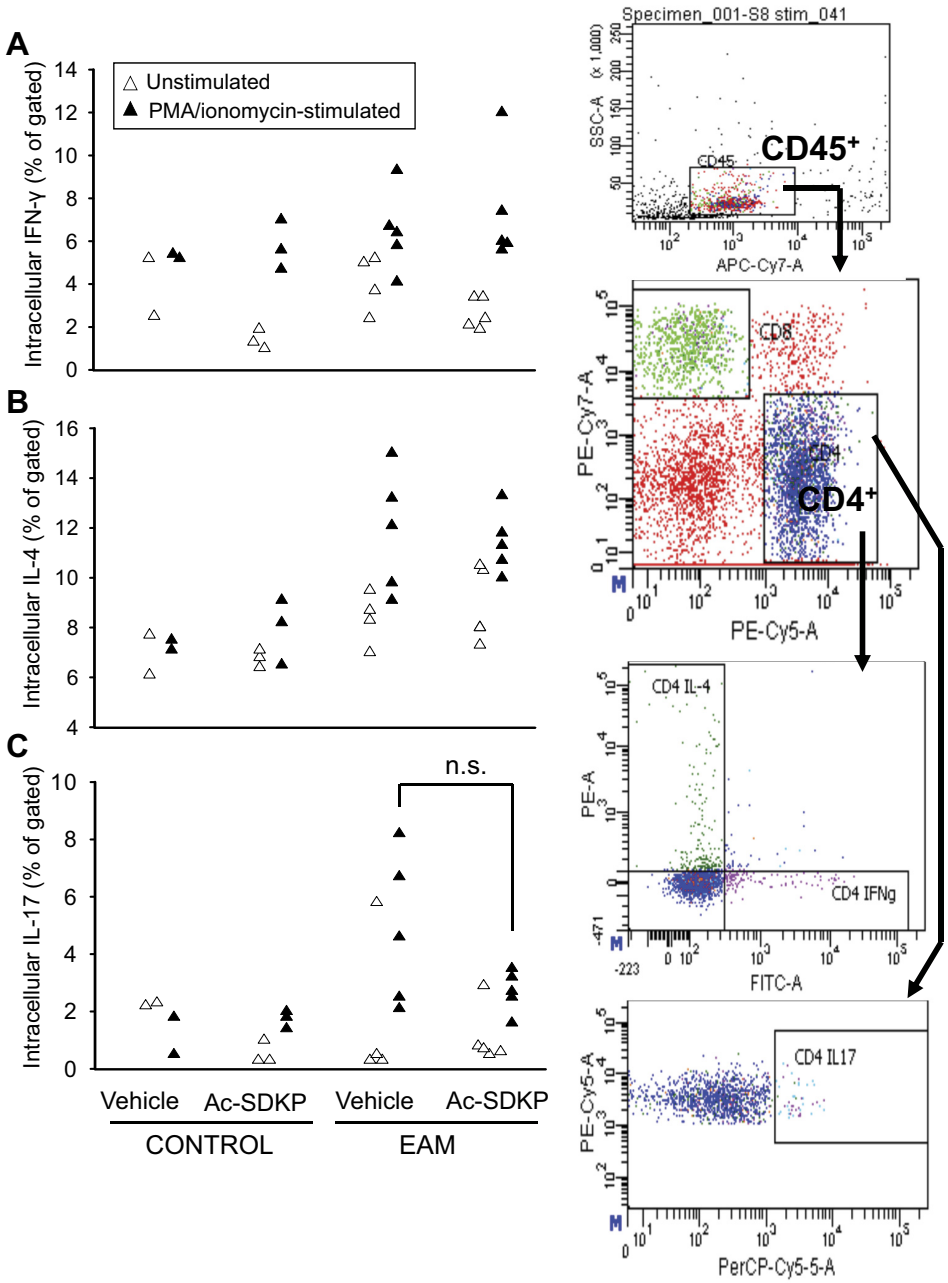

Fig. 6. *Left*: quantification of interferon-γ (IFN-γ)-positive (+) (*A*), interleukin (IL)-4$^+$ (*B*), and IL-17$^+$ (*C*) T helper cells in a population of lymph node cells under unstimulated (open triangles) and phorbol 12-myristate 13-acetate (PMA)/ionomycin-stimulated conditions (closed triangles) in controls and EAM rats treated with vehicle or Ac-SDKP. *Right*: figure showing gating strategy in a representative sample for the analysis of different T helper cell subsets in CD45$^+$ and CD4$^+$ events. Total leukocytes were gated on using CD45 expression and side scatter properties. Subsequently, CD45$^+$ cells were gated on CD4$^+$ and CD8$^+$ cells, which were subsequently analyzed for IL-4, IFN-γ, and IL-17 expression.

myocardial injury, Ac-SDKP prevents not only cardiac inflammation and fibrosis but also hypertrophy along with systolic and diastolic dysfunction. It would be tempting to postulate that the reduced cardiac fibrosis was responsible for the improved diastolic dysfunction in the rats treated with Ac-SDKP; however, in an earlier study, we found that spontaneously hypertensive rats treated with Ac-SDKP had reduced cardiac fibrosis without improved hypertrophy or altered diastolic function despite decreased systolic function (8). Thus we believe prevention of systolic and diastolic dysfunction in animals with EAM treated with Ac-SDKP may be attributable to simultaneous protection against multiple pathogenetic factors, including hypertrophy, fibrosis, and inflammation.

Improved cardiac function and reduced hypertrophy were accompanied by decreased inflammation. The grade of inflammation observed in this study was comparable with other group's reports (43). We previously showed that Ac-SDKP reduces mast cell and macrophage infiltration (24), and now we can report it also prevents dendritic cell and T helper cell infiltration; this is important because both are key components of the innate and adaptive arms of the immune system. Although Ac-SDKP did not reduce CD8$^+$ T cells in the EAM group, it is well recognized that in these rats CD4$^+$ are more important than CD8$^+$ (6, 20, 26, 43). There is substantial evidence that innate immune cytokines such as TNF-α and IL-1 are crucial for the onset of autoimmunity, so that resistant strains become susceptible when treated with IL-1 or TNF-α (21). TNF-rp 55 knockout animals do not develop EAM (3), and neutralization of TNF with monoclonal antibodies ameliorates the disease (38). In our study, the cardiac cytokine

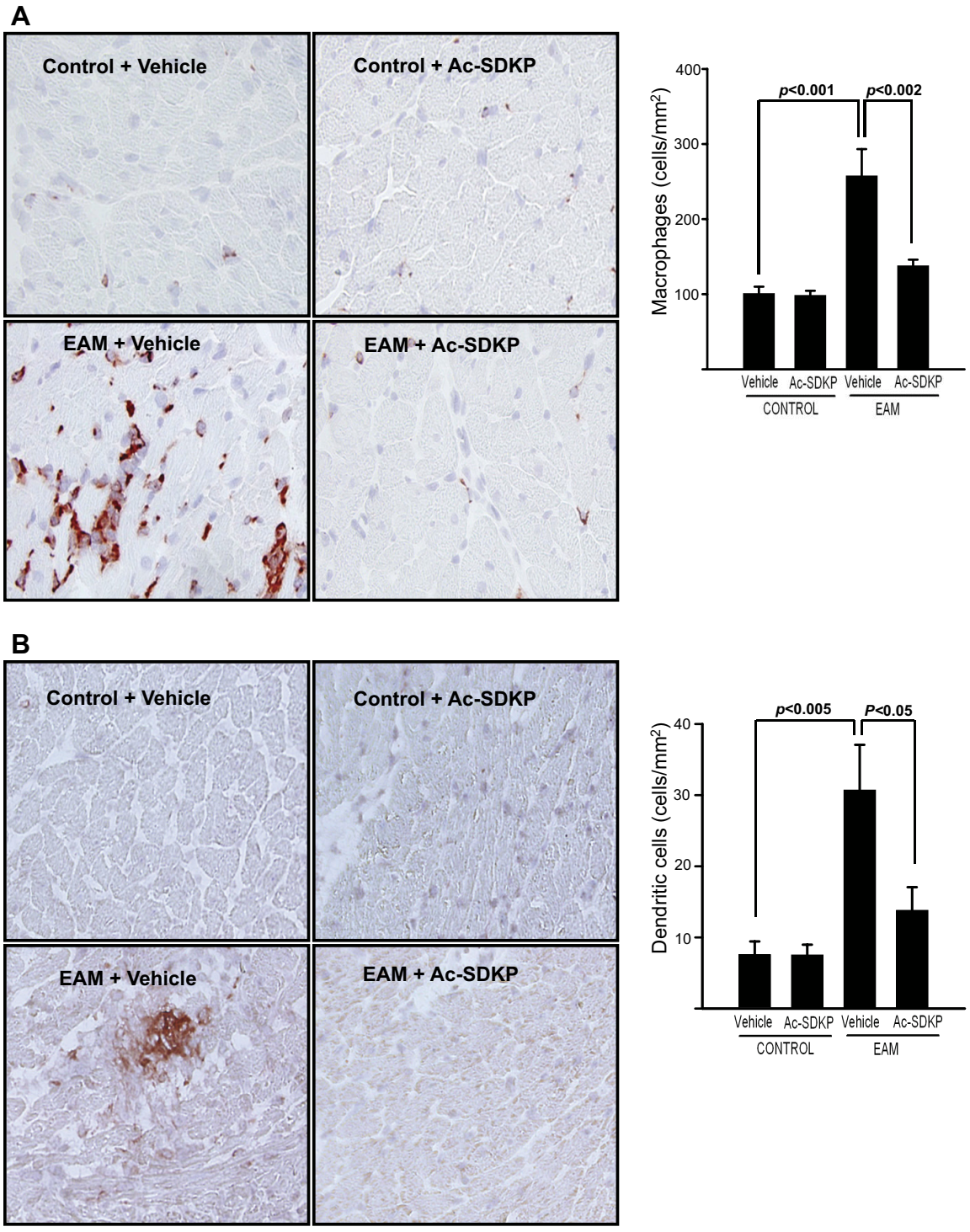

Fig. 7. *A*: *left*, representative images of myocardial macrophage infiltration (red: ED-1 positive) 4 wk after immunization in controls and EAM rats treated with vehicle or Ac-SDKP. *Right*, quantitative data, expressed as cells/mm^2 (n = 11–13). *B*: *left*, representative images of myocardial dendritic cell infiltration (red: CD11c positive) 3 wk after immunization in controls and EAM rats treated with vehicle or Ac-SDKP. *Right*, quantitative data, expressed as cells/mm^2 (n= 7–8).

expression profile revealed that, in EAM, Ac-SDKP prevented increases in cytokines related to innate (IL-1α and -β, IL-6, and TNF-α) and adaptive [IL-2, IP-10 (Th1 activation marker), and IL-17 (Th17 activation marker)] immune activation. Han et al. (13) determined that the Th1 response is associated with the initial cellular inflammatory stage of myocarditis, whereas Th2 predominates during the chronic stages when fibrosis is exacerbated; in turn, Baldeviano et al. (5) reported that Th17 is not required for myocarditis but essential for progression to dilated cardiomyopathy. We identified T subsets in the lymph nodes by FACS and found that Th1 was not altered in EAM 3 wk postimmunization; nevertheless, we cannot rule out the possibility that it is increased earlier than 3 wk. As we expected, Th2 and T17 subsets tended to be higher at 3 wk in

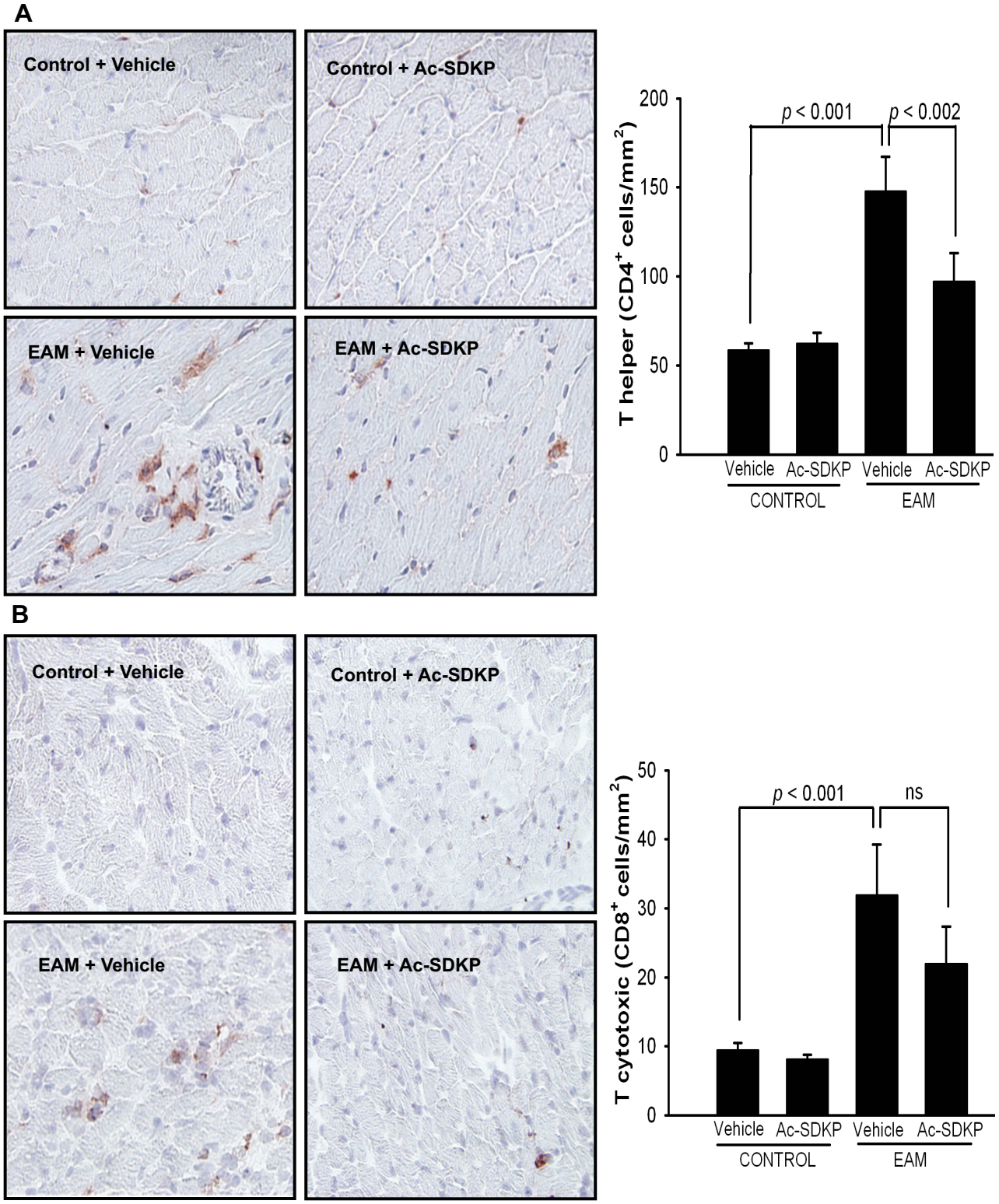

Fig. 8. *Left*: representative images of myocardial T helper cell (red: CD4 positive) (*A*) and T cytotoxic infiltration (red: CD8 positive) (*B*) in controls and EAM rats treated with vehicle or Ac-SDKP 4 wk after immunization. *Right*: quantitative data, expressed as cells/mm^2 (n = 10–14).

EAM; and, although Ac-SDKP had no effect on Th2, it tended to prevent an increase in Th17. Taken together, we speculate that the inhibitory effects of Ac-SDKP on Th17 and IL-17 expression may protect against postmyocarditis remodeling and progression to DCM during the chronic stage of the disease.

Ac-SDKP prevented expression of the chemokines CINC-1 and IP-10 in cardiac tissue. CINC-1 has been

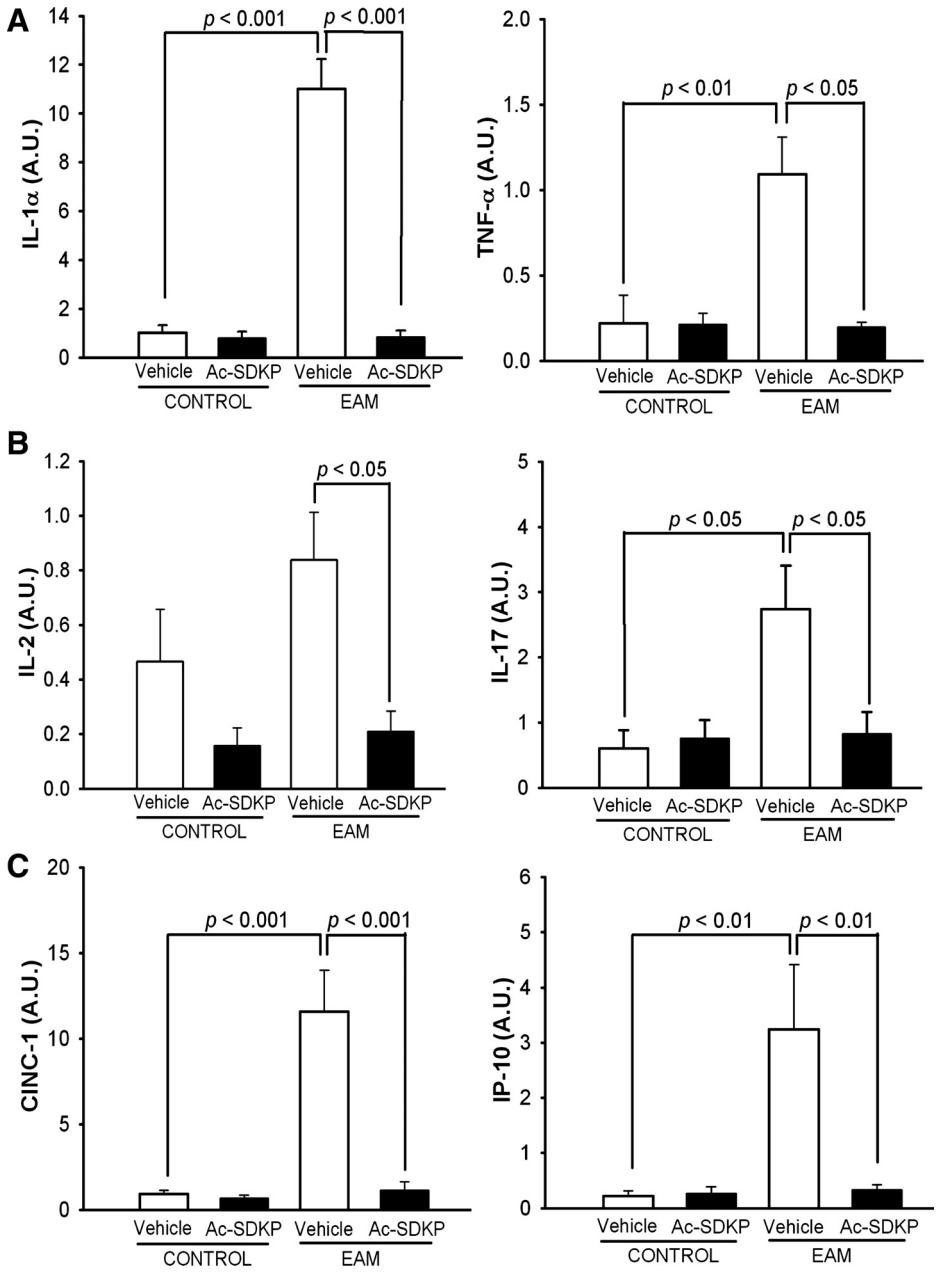

Fig. 9. Expression of cytokines related to innate immunity [IL-1α, tumor necrosis factor (TNF)-α] (*A*), cytokines related to adaptive immunity (IL-2 and IL-17) (*B*), and chemokines [cytokine-induced neutrophil chemoattractant-1 (CINC-1), interferon-γ-induced protein 10 (IP-10)] (*C*) measured with a commercially available rat cytokine array kit 3 wk after immunization in hearts from controls and EAM rats treated with vehicle or Ac-SDKP ($n = 5$).

posited as a critical mediator of neutrophil infiltration in rats during inflammation (14), whereas IP-10 is induced in many cells in response to interferon-γ (25) and is also seen in Th1-type inflammatory diseases where it is thought to play an important role in recruiting activated T cells into sites of inflammation (10).

It is also well-established that the recruitment of leukocytes to the inflammatory sites requires the binding to cell adhesion molecules. Treatment with Ac-SDKP reduced the protein expression of L-selectin and ICAM-1. It has been shown that expression of endothelial ICAM-1 is a prerequisite for target organ recognition by autoreactive T cells in CD4-mediated myocarditis as reported by Pummerer et al. (33).

MMPs are also considered crucial to recruitment of inflammatory cells and cardiac remodeling (15, 18, 39). Because Hishikari et al. (16) indicated EAM can be prevented by blocking MMPs, we studied the effect of Ac-SDKP on MMP activity. Measurement of MMP-2 and MMP-9 by zymography showed both enzymes were increased by 2 wk in the EAM group, and this increase was prevented by Ac-SDKP; thus, we believe Ac-SDKP may decrease infiltration by immune cells (and later cytokine production) in part by decreasing MMPs in addition to chemokines and cell adhesion molecules.

When we evaluated cell-mediated immunity by DTH, ear swelling was reduced in EAM rats treated with Ac-SDKP. Since Volkov et al. (41) demonstrated that adding Ac-SDKP to cultured T cells in vitro blocked the proliferation induced by concanavalin A, phytohemagglutinin, and pokeweed mitogen, and, since Ac-SDKP was initially described as a physiological negative regulator of hematopoietic stem cell proliferation (22), the decrease in DTH led us to hypothesize that Ac-SDKP blunts development of autoreactive T cells, possibly accompa-

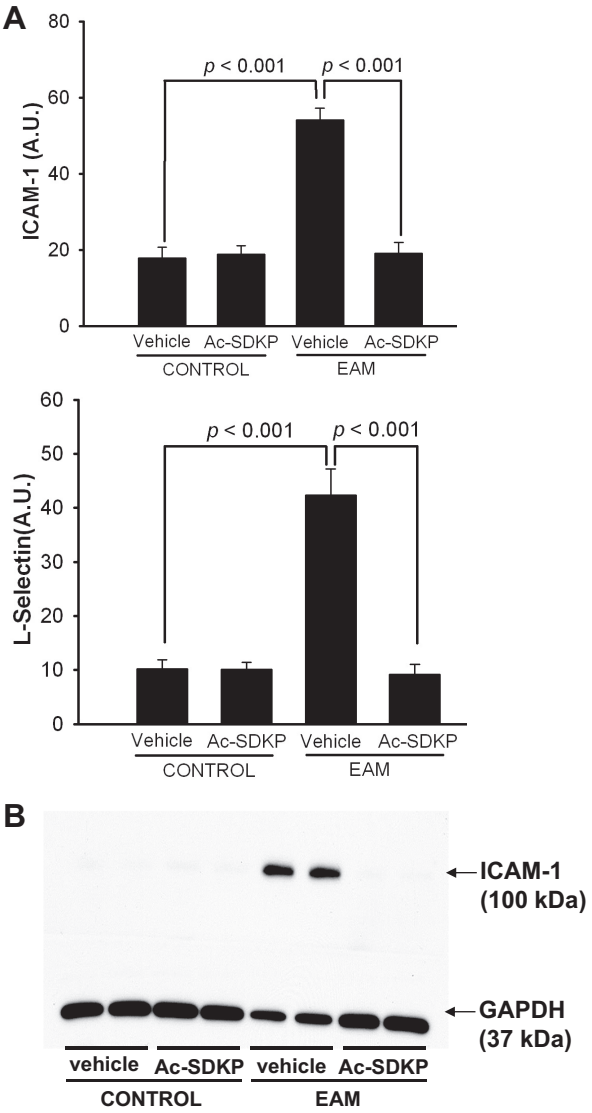

Fig. 10. *A*: expression of intercellular adhesion molecule (ICAM)-1 and L-selectin measured with a commercially available rat cytokine array kit 3 wk after immunization in hearts from controls and EAM rats treated with vehicle or Ac-SDKP ($n = 5$). *B*: representative images of ICAM-1 expression measured by Western blot in hearts from controls and EAM rats treated with vehicle or Ac-SDKP ($n = 5$).

nied by reduced autoantibody titers. We measured antigen-specific T cell responses by FACS and cardiac myosin-specific autoantibodies by ELISA and were surprised to find that Ac-SDKP not only failed to prevent autoantibody production but also fell short of lowering antigen-specific T cell responses, suggesting that, in this model, Ac-SDKP prevents cardiac damage primarily by reducing the local proinflammatory environment rather than preventing autoantibody production and/or development of autoreactive T cells. Because Ac-SDKP has been shown to have direct effects on macrophages by reducing TNF-α release and trafficking (35), we believe it decreased DTH by acting directly on macrophages rather than T cells or dendritic cells.

From these observations, we conclude that Ac-SDKP may not prevent the development of autoreactive cells that initiate autoimmunity, but instead Ac-SDKP acts at a different level by blocking the infiltration by these cells and other effector cells that trigger cardiac injury. These effects of Ac-SDKP are likely mediated by reduction of cytokines, chemokines, adhesion molecules, and MMPs, resulting in improvement of cardiac function and reduction of cardiac remodeling.

Perspectives

We believe our data demonstrate for the first time that Ac-SDKP, a naturally occurring tetrapeptide, exerts protective effects in autoimmune-mediated cardiac diseases. Ac-SDKP or analogs resistant to peptidases could be used to treat diseases in which autoimmunity plays a pathogenic role, such as systemic lupus erythematosus, rheumatoid arthritis, multiple sclerosis, organ rejection, diabetes mellitus type 1, atherosclerosis, and hypertensive target organ damage. Also, because ACE inhibitors can protect against autoimmune diseases (11, 36) including EAM (11), and since Ac-SDKP is specifically degraded by ACE as supported by the observation that ACE inhibitors significantly increase Ac-SDKP in plasma and urine (1, 2), we believe increased Ac-SDKP may explain some of the beneficial effects of ACE inhibitors.

ACKNOWLEDGMENTS

We wish to thank Gulser Gurocak for her technical expertise and Elizabeth Furest and Tasnim Hoda for their exceptional editing assistance.

GRANTS

This work was supported by National Heart, Lung, and Blood Institute Grants HL-028982 and HL-088036 to O. A. Carretero and HL-071806 to N.-E. Rhaleb.

DISCLOSURES

No conflicts of interest, financial or otherwise, are declared by the authors.

AUTHOR CONTRIBUTIONS

Author contributions: P.N., Y.-H.L., T.-D.L., G.E.G., and O.A.C. conception and design of research; P.N., Y.-H.L., T.-D.L., X.C., and D.S. performed experiments; P.N., Y.-H.L., T.-D.L., E.L.P., and O.A.C. analyzed data; P.N., Y.-H.L., K.R.B., X.-P.Y., N.-E.R., and O.A.C. interpreted results of experiments; P.N. and Y.-H.L. prepared figures; P.N. drafted manuscript; P.N., Y.-H.L., K.R.B., D.S., R.K., X.-P.Y., N.-E.R., and O.A.C. edited and revised manuscript; P.N., Y.-H.L., T.-D.L., X.C., G.E.G., K.R.B., D.S., E.L.P., R.K., X.-P.Y., N.-E.R., and O.A.C. approved final version of manuscript.

REFERENCES

1. **Azizi M, Ezan E, Nicolet L, Grognet JM, Ménard J.** High plasma level of N-acetyl-seryl-aspartyl-lysyl-proline: a new marker of chronic angiotensin-converting enzyme inhibition. *Hypertension* 30: 1015–1019, 1997.
2. **Azizi M, Rousseau A, Ezan E, Guyene TT, Michelet S, Grognet JM, Lenfant M, Corvol P, Menard J.** Acute angiotensin-converting enzyme inhibition increases the plasma level of the natural stem cell regulator N-acetyl-seryl-aspartyl-lysyl-proline. *JCI* 97: 839–844, 1996.
3. **Bachmaier K, Pummerer C, Kozieradzki I, Pfeffer K, Mak TW, Neu N, Penninger JM.** Low-molecular-weight tumor necrosis factor receptor p55 controls induction of autoimmune heart disease. *Circulation* 95: 655–661, 1997.
4. **Bahk TJ, Daniels MD, Leon JS, Wang K, Engman DM.** Comparison of angiotensin converting enzyme inhibition and angiotensin II receptor blockade for the prevention of experimental autoimmune myocarditis. *Int J Cardiol* 125: 85–93, 2008.
5. **Baldeviano GC, Barin JG, Talor MV, Srinivasan S, Bedja D, Zheng D, Gabrielson K, Iwakura Y, Rose NR, Cihakova D.** Interleukin-17A is dispensable for myocarditis but essential for the progression to dilated cardiomyopathy. *Circ Res* 106: 1646–1655, 2010.
6. **Blyszczuk P, Kania G, Dieterle T, Marty RR, Valaperti A, Berthonneche C, Pedrazzini T, Berger CT, Dirnhofer S, Matter CM, Pen-**

Table 3. *Additional inflammatory mediators measured 3 wk after immunization in heart homogenates from controls and EAM rats treated with vehicle or Ac-SDKP*

Protein	Control	Ac-SDKP	EAM	EAM+Ac-SDKP
CINC-2 α/β	0.24 ± 0.04	0.29 ± 0.12	0.57 ± 0.10	0.08 ± 0.05
CINC-3	0.82 ± 0.24	0.45 ± 0.13	1.46 ± 0.30	0.58 ± 0.21#
CNTF	0.45 ± 0.12	0.28 ± 0.08	0.55 ± 0.14	0.24 ± 0.07
Fractalkine	1.35 ± 0.30	1.11 ± 0.30	1.62 ± 0.37	1.10 ± 0.35
GM-CSF	1.32 ± 0.73	0.73 ± 0.32	0.91 ± 0.34	0.47 ± 0.16
IFN-γ	0.85 ± 0.20	0.69 ± 0.23	0.96 ± 0.21	0.87 ± 0.20
IL-1β	0.35 ± 0.11	0.50 ± 0.19	1.76 ± 0.35**	0.29 ± 0.07###
IL-1ra	0.30 ± 0.10	0.23 ± 0.10	19.96 ± 7.45*	0.30 ± 0.12#
IL-3	0.57 ± 0.16	0.56 ± 0.18	1.28 ± 0.28	0.29 ± 0.08
IL-4	0.50 ± 0.14	0.57 ± 0.16	0.60 ± 0.18	0.28 ± 0.10
IL-6	1.01 ± 0.23	0.71 ± 0.17	1.56 ± 0.21	0.72 ± 0.17#
IL-10	0.66 ± 0.20	0.49 ± 0.10	0.57 ± 0.11	0.67 ± 0.20
IL-13	0.70 ± 0.22	0.55 ± 0.16	1.01 ± 0.23	0.67 ± 0.17
LIX	1.16 ± 0.31	1.03 ± 0.24	19.61 ± 5.78*	1.02 ± 0.25##
MIG	0.84 ± 0.21	0.69 ± 0.15	3.29 ± 1.30	0.57 ± 0.15
MIP-1α	0.40 ± 0.21	0.19 ± 0.07	1.54 ± 0.23**	0.24 ± 0.09###
MIP-3α	0.55 ± 0.28	0.35 ± 0.08	1.14 ± 0.19	0.61 ± 0.32
RANTES	2.23 ± 0.55	1.97 ± 0.38	5.22 ± 1.71	2.29 ± 0.62
Thymus chemokine	37.33 ± 2.90	38.42 ± 5.66	53.09 ± 3.20	33.19 ± 5.01#
TIMP-1	0.52 ± 0.08	0.45 ± 0.09	66.30 ± 14.15**	1.06 ± 0.51###
VEGF	1.82 ± 0.64	1.98 ± 0.61	2.83 ± 0.50	1.24 ± 0.21

Values are means ± SE. CINC, cytokine-induced neutrophil chemoattractant; CNTF, cilliary neurotrophic factor; GM-CSF, granulocyte macrophage colny-stimulating factor; IFN, interferon; IL, interleukin; ra, receptor antagonist; LIX, lipopolysaccharide-induced CXC chemokine; MIG, MIP. macrophage inflammatory protein; RANTES, rapid upon activation normal T cell expressed and secreted; TIMP, tissue inhibitor of metalloproteinase; VEGF, vascular endothelial growth factor. *$P < 0.005$ and **$P < 0.001$, EAM vs. control. #$P < 0.05$, ##$P < 0.005$, and ###$P < 0.001$, EAM+Ac-SDKP vs. EAM.

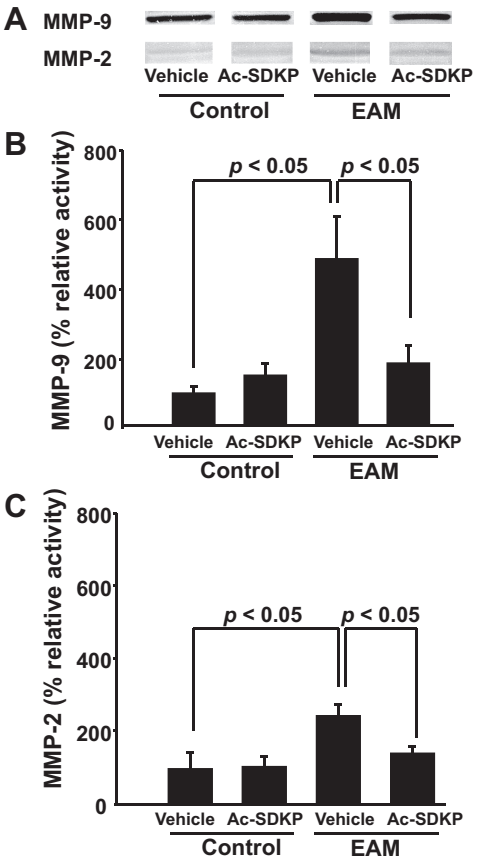

Fig. 11. *A*: representative images showing matrix metalloproteinase (MMP)-9 (*top*) and MMP-2 (*bottom*) activity measured by zymography 2 wk after immunization in hearts of controls and EAM rats treated with vehicle or Ac-SDKP. Quantitative data on MMP-9 (*B*) and MMP-2 (*C*) activity are expressed as a percentage of control ($n = 3–6$).

ninger JM, Lüscher TF, Eriksson U. Myeloid differentiation factor-88/interleukin-1 signaling controls cardiac fibrosis and heart failure progression in inflammatory dilated cardiomyopathy. *Circ Res* 105: 912–920, 2009.

7. **Cavasin MA, Rhaleb NE, Yang XP, Carretero OA.** Prolyl oligopeptidase is involved in release of the antifibrotic peptide Ac-SDKP. *Hypertension* 43: 1140–1145, 2004.
8. **Cingolani OH, Yang XP, Liu YH, Villanueva M, Rhaleb NE, Carretero OA.** Reduction of cardiac fibrosis decreases systolic performance without affecting diastolic function in hypertensive rats. *Hypertension* 43: 1067–1073, 2004.
9. **Damoiseaux JG, Döpp EA, Calame W, Chao D, MacPherson GG, Dijkstra CD.** Rat macrophage lysosomal membrane antigen recognized by monoclonal antibody ED1. *Immunology* 83: 140–147, 1994.
10. **Dufour JH, Dziejman M, Liu MT, Leung JH, Lane TE, Luster AD.** IFN-gamma-inducible protein 10 (IP-10; CXCL10)-deficient mice reveal a role for IP-10 in effector T cell generation and trafficking. *J Immunol* 168: 3195–3204, 2002.
11. **Godsel LM, Leon JS, Wang K, Fornek JL, Molteni A, Engman DM.** Captopril prevents experimental autoimmune myocarditis. *J Immunol* 171: 346–352, 2003.
12. **Goser S, Ottl R, Brodner A, Dengler TJ, Torzewski J, Egashira K, Rose NR, Katus HA, Kaya Z.** Critical role for monocyte chemoattractant protein-1 and macrophage inflammatory protein-1alpha in induction of experimental autoimmune myocarditis and effective anti-monocyte chemoattractant protein-1 gene therapy. *Circulation* 112: 3400–3407, 2005.
13. **Han LN, Li TL, Zhang YJ, Yang TS, Ding Y, Guo SL.** Immune state of Th1, Th2 and Th17 subpopulation in experimental autoimmune myocarditis. *Sichuan Da Xue Xue Bao Yi Xue Ban* 42: 751–756, 2011.
14. **Handa O, Naito Y, Takagi T, Shimozawa M, Kokura S, Yoshida N, Matsui H, Cepinskas G, Kvietys PR, Yoshikawa T.** Tumor necrosis factor-alpha-induced cytokine-induced neutrophil chemoattractant-1 (CINC-1) production by rat gastric epithelial cells: role of reactive oxygen species and nuclear factor-kappaB. *J Pharmacol Exp Ther* 309: 670–676, 2004.
15. **Heymans S, Pauschinger M, DePalma A, Kallwellis-Opara A, Rutschow S, Swinnen M, Vanhoutte D, Gao F, Torpai R, Baker AH, Padalko E, Neyts J, Schultheiss HP, Van de Werf F, Carmeliet P, Pinto YM.** Inhibition of urokinase-type plasminogen activator or matrix metalloproteinases prevents cardiac injury and dysfunction during viral myocarditis. *Circulation* 114: 565–573, 2006.

16. **Hishikari K, Watanabe R, Ogawa M, Suzuki J, Masumura M, Shimizu T, Takayama K, Hirata Y, Nagai R, Isobe M.** Early treatment with clarithromycin attenuates rat autoimmune myocarditis via inhibition of matrix metalloproteinase activity. *Heart* 96: 523–527, 2010.
17. **Kitabayashi H, Isobe M, Watanabe N, Suzuki J, Yazaki Y, Sekiguchi M.** FTY720 prevents development of experimental autoimmune myocarditis through reduction of circulating lymphocytes. *J Cardiovasc Pharmacol* 35: 410–416, 2000.
18. **Kodama M, Hanawa H, Saeki M, Hosono H, Inomata T, Suzuki K, Shibata A.** Rat dilated cardiomyopathy after autoimmune giant cell myocarditis. *Circ Res* 75: 278–284, 1994.
19. **Kodama M, Matsumoto Y, Fujiwara M.** In vivo lymphocyte-mediated myocardial injuries demonstrated by adoptive transfer of experimental autoimmune myocarditis. *Circulation* 85: 1918–1926, 1992.
20. **Kodama M, Zhang S, Hanawa H, Shibata A.** Immunohistochemical characterization of infiltrating mononuclear cells in the rat heart with experimental autoimmune giant cell myocarditis. *Clin Exp Immunol* 90: 330–335, 1992.
21. **Lane JR, Neumann DA, Lafond-Walker A, Herskowitz A, Rose NR.** Role of IL-1 and tumor necrosis factor in coxsackie virus-induced autoimmune myocarditis. *J Immunol* 151: 1682–1690, 1993.
22. **Lenfant M, Wdzieczak-Bakala J, Guittet E, Prome JC, Sotty D, Frindel E.** Inhibitor of hematopoietic pluripotent stem cell proliferation: purification and determination of its structure. *Proc Natl Acad Sci USA* 86: 779–782, 1989.
23. **Liu W, Li WM, Gao C, Sun NL.** Effects of atorvastatin on the Th1/Th2 polarization of ongoing experimental autoimmune myocarditis in Lewis rats. *J Autoimmun* 25: 258–263, 2005.
24. **Liu YH, D'Ambrosio M, Liao TD, Peng H, Rhaleb NE, Sharma U, André S, Gabius HJ, Carretero OA.** N-acetyl-seryl-aspartyl-lysyl-proline prevents cardiac remodeling and dysfunction induced by galectin-3, a mammalian adhesion/growth-regulatory lectin. *Am J Physiol Heart Circ Physiol* 296: H404–H412, 2009.
25. **Luster AD, Greenberg SM, Leder P.** The IP-10 chemokine binds to a specific cell surface heparan sulfate site shared with platelet factor 4 and inhibits endothelial cell proliferation. *J Exp Med* 182: 219–231, 1995.
26. **Marino AP, Azevedo MI, Lannes-Vieira J.** Differential expression of adhesion moleculesshaping the T-cell subset prevalence during the early phase of autoimmune and Trypanosoma cruzi-elicited myocarditis. *Mem Inst Oswaldo Cruz* 98: 945–952, 2003.
27. **Peng H, Carretero OA, Brigstock DR, Oja-Tebbe N, Rhaleb NE.** Ac-SDKP reverses cardiac fibrosis in rats with renovascular hypertension. *Hypertension* 42: 1164–1170, 2003.
28. **Peng H, Carretero OA, Liao TD, Peterson EL, Rhaleb NE.** Role of N-acetyl-seryl-aspartyl-lysyl-proline in the antifibrotic and anti-inflammatory effects of the angiotensin-converting enzyme inhibitor captopril in hypertension. *Hypertension* 49: 695–703, 2007.
29. **Peng H, Carretero OA, Raij L, Yang F, Kapke A, Rhaleb NE.** Antifibrotic effects of *N*-acetyl-seryl-aspartyl-lysyl-proline on the heart and kidney in aldosterone-salt hypertensive rats. *Hypertension* 37: 794–800, 2001.
30. **Peng H, Carretero OA, Vuljaj N, Liao TD, Motivala A, Peterson EL, Rhaleb NE.** Angiotensin-converting enzyme inhibitors: a new mechanism of action. *Circulation* 112: 2436–2445, 2005.
31. **Pokharel S, van Geel PP, Sharma UC, Cleutjens JPM, Bohnemeier H, Tian XL, Schunkert H, Crijns HJGM, Paul M, Pinto YM.** Increased myocardial collagen content in transgenic rats overexpressing cardiac angiotensin-converting enzyme is related to enhanced breakdown of *N*-acetyl-Ser-Asp-Lys-Pro and increased phosphorylation of Smad2/3. *Circulation* 110: 3129–3135, 2004.
32. **Prunier F, Gaertner R, Louedec L, Michel JB, Mercadier JJ, Escoubet B.** Doppler echocardiographic estimation of left ventricular end-diastolic pressure after MI in rats. *Am J Physiol Heart Circ Physiol* 283: H346–H352, 2002.
33. **Pummerer CL, Grassl G, Sailer M, Bachmaier KW, Penninger JM, Neu N.** Cardiac myosin-induced myocarditis: target recognition by autoreactive T cells requires prior activation of cardiac interstitial cells. *Lab Invest* 74: 845–852, 1996.
34. **Rhaleb NE, Peng H, Yang XP, Liu YH, Mehta D, Ezan E, Carretero OA.** Long-term effect of N-acetyl-seryl-aspartyl-lysyl-proline on left ventricular collagen deposition in rats with 2-kidney, 1-clip hypertension. *Circulation* 103: 3136–3141, 2001.
35. **Sharma U, Rhaleb NE, Pokharel S, Harding P, Rasoul S, Peng H, Carretero OA.** Novel anti-inflammatory mechanisms of N-Acetyl-Ser-Asp-Lys-Pro in hypertension-induced target organ damage. *Am J Physiol Heart Circ Physiol* 294: H1226–H1232, 2008.
36. **Shimazu H, Kinoshita K, Hino S, Yano T, Kishimoto K, Nagare Y, Nozaki Y, Sugiyama M, Ikoma S, Funauchi M.** Effect of combining ACE inhibitor and statin in lupus-prone mice. *Clin Immunol* 136: 188–196, 2010.
37. **Smith SC, Allen PM.** Myosin-induced acute myocarditis is a T cell-mediated disease. *J Immunol* 147: 2141–2147, 1991.
38. **Smith SC, Allen PM.** Neutralization of endogenous tumor necrosis factor ameliorates the severity of myosin-induced myocarditis. *Circ Res* 70: 856–863, 1992.
39. **Spinale FG.** Myocardial matrix remodeling and the matrix metalloproteinases: influence on cardiac form and function. *Physiol Rev* 87: 1285–1342, 2007.
40. **Sweat F, Puchtler H, Rosenthal SI.** Sirius Red F3BA as a stain for connective tissue. *Arch Pathol* 78: 69–72, 1964.
41. **Volkov L, Quere P, Coudert F, Comte L, Praloran V.** The tetrapeptide AcSDKP, a physiological inhibitor of normal cell proliferation, reduces the S phase entry of continuous cell lines. *Exp Cell Res* 223: 112–116, 1996.
42. **Wang QQ, Wang YL, Yuan HT, Liu FQ, Jin YP, Han B.** Immune tolerance to cardiac myosin induced by anti-CD4 monoclonal antibody in autoimmune myocarditis rats. *J Clin Immunol* 26: 213–221, 2006.
43. **Wang Y, Afanasyeva M, Hill SL, Rose NR.** Characterization of murine autoimmune myocarditis induced by self and foreign cardiac myosin. *Autoimmunity* 31: 151–162, 1999.
44. **Yang F, Yang XP, Liu YH, Xu J, Cingolani O, Rhaleb NE, Carretero OA.** Ac-SDKP reverses inflammation and fibrosis in rats with heart failure after myocardial infarction. *Hypertension* 43: 229–236, 2004.
45. **Zibadi S, Vazquez R, Moore D, Larson DF, Watson RR.** Myocardial lysyl oxidase regulation of cardiac remodeling in a murine model of diet-induced metabolic syndrome. *Am J Physiol Heart Circ Physiol* 297: H976–H982, 2009.